PERGAMON

International Journal of Heat and Mass Transfer 45 (2002) 963–977

International Journal of HEAT and MASS TRANSFER

www.elsevier.com/locate/ijhmt

Laminar free-convection over a vertical isothermal plate with uniform blowing or suction in water with variable physical properties

A. Pantokratoras *

School of Engineering, Democritus University of Thrace, 67100 Xanthi, Greece

Received 19 February 2001; received in revised form 1 July 2001

Abstract

The majority of studies for laminar free-convection over a vertical isothermal plate with uniform blowing or suction concern gases and air. The existing results for water have been produced assuming a linear relationship between fluid density and temperature and constant viscosity and thermal conductivity. However, it is known that the density–temperature relationship for water is non-linear at low temperatures and viscosity and thermal conductivity are functions of temperature. In this study the problem of laminar free-convection over a vertical isothermal plate with uniform blowing or suction in water has been investigated in the temperature range between 20 and 0 °C taking into account the temperature-dependence of μ, k and ρ. The results are obtained with the numerical solution of the boundary layer equations. The variation of μ, k and ρ with temperature has a strong influence on the results. © 2002 Published by Elsevier Science Ltd.

1. Introduction

Free-convection along a vertical plate with mass transfer at the wall has been studied by many authors in the past. Eichhorn [5] was the first to study the effect of suction and injection on free-convective flow. He considered power-law variations of plate temperature ($T_0 = c_1 x^m$) and transpiration velocity ($v_0 = c_2 x^{(m-1)/4}$) under which self-similar solutions of the governing equations are possible and presented results for constant temperature plate ($m = 0$) and variable transpiration velocity ($v_0 = c_2 x^{-1/4}$) for a fluid with $Pr = 0.73$. For the case of isothermal plate with uniform blowing or suction similarity solutions do not exist. For the latter problem Sparrow and Cess [17] provided approximate series solutions valid near the plate leading edge for $Pr = 0.72$. This problem was considered in more detail by Merkin [10] who obtained asymptotic solutions, valid at large distances from the leading edge, and presented results for $Pr = 1$. The next order corrections to the boundary layer solution for this problem, concerning gases, were obtained by Clarke [4] who did not invoke the usual Boussinesq approximation. The solutions for strong suction and blowing on general body shapes which admit a similarity solution has been given by Merkin [11]. Parikh et al. [16] studied both numerically and experimentally the problem of air ($Pr = 0.7$) free-convection over an isothermal porous vertical plate with uniform transpiration taking into account the air variable physical properties. Minkowycz and Sparrow [13] using the local non-similarity method presented solutions for a wide range of Pr numbers ($Pr = 0.01$, 0.02, 0.05, 0.10, 0.20, 0.50, 0.70, 0.72, 1.0, 2.0, 5.0, 10.0, 20.0, 50.0, 100.0). Vedhanayagam et al. [19] presented a transformation of the equations for general blowing and wall temperature variations and presented results for the isothermal plate with uniform blowing for $Pr = 0.7$. A solution to the constant plate temperature with uniform air blowing, based on the film model, has been derived by Brouwers [1]. In a subsequent paper Brouwers [2], using the film model, derived a thermal correction factor and a novel friction correction factor which were applied to free-

* Tel.: +541-79618.

E-mail address: apantokr@civil.duth.gr (A. Pantokratoras).

0017-9310/02/$ - see front matter © 2002 Published by Elsevier Science Ltd.
PII: S0017-9310(01)00208-3

Nomenclature

c_p	water specific heat (J kg^{-1} °C^{-1})
f	dimensionless stream function
g	gravitational acceleration (m s^{-2})
Gr_x	local Grashof number
k	thermal conductivity (J s^{-1} m^{-1} °C^{-1})
Nu_x	local Nusselt number
Nu_x^*	local Nusselt number with zero transpiration
p	pressure (N m^{-2})
Pr	Prandtl number
Pr_a	ambient Prandtl number
s	salinity
T	water temperature (°C)
T_a	ambient water temperature (°C)
T_0	plate temperature (°C)
u	vertical velocity (m s^{-1})
v	horizontal velocity (m s^{-1})
v_0	transpiration velocity (m s^{-1})
x	vertical coordinate (m)
y	horizontal coordinate (m)

Greek symbols

β	thermal expansion coefficient of water
n	pseudo-similarity variable
μ	dynamic viscosity (kg m^{-1} s)
μ_f	film dynamic viscosity (kg m^{-1} s)
μ_0	dynamic viscosity at plate (kg m^{-1} s)
ν	kinematic viscosity (m^2 s^{-1})
ξ	injection parameter
ρ	water density (kg m^{-3})
ρ_a	ambient water density (kg m^{-3})
ρ_f	film water density (kg m^{-3})
ρ_0	water density at plate (kg m^{-3})
φ	non-dimensional temperature

convection along a vertical porous plate for $Pr = 0.73$, 1 and 7. The problem of blowing and suction on the free-convection over a vertical plate with a given wall heat flux has been considered by Chaudhary and Merkin [3]. The presented results are valid for $Pr = 1$. Merkin [12] considered again the problem of free-convection flow on a vertical plate with prescribed temperature and presented results for variable transpiration velocities for Pr numbers 1 and 7.

From the above literature review it is clear that for laminar free-convection over a vertical isothermal plate with constant blowing or suction the only results that correspond to water are those of Minkowycz and Sparrow [13] and specifically the results for $Pr = 5$ and 10. It should be mentioned here that $Pr = 5$ corresponds to water temperature equal to 32.78 °C and $Pr = 10$ to 7.78 °C. In addition, only two of the above works take into account the temperature-dependence of the fluid physical properties [4,16]. These works concern gases and air. However, it is known that the temperature-dependence of fluid properties (dynamic viscosity, thermal conductivity and density) is quite different in air from that in water. For example, the viscosity of air increases with temperature, whereas water viscosity decreases with temperature. Therefore, for heating a fluid, the effect of temperature-dependent viscosity is to decrease transport in air and to increase transport in water. The opposite occurs for cooling the fluid. On the other hand, the density–temperature relationship is linear for air whereas in water this relationship is linear at high temperatures and non-linear at low temperatures (see Fig. 1). The density of pure water is maximum at 3.98 °C. The density increases as the temperatures decreases approaching 3.98 °C, while the density decreases as the temperature

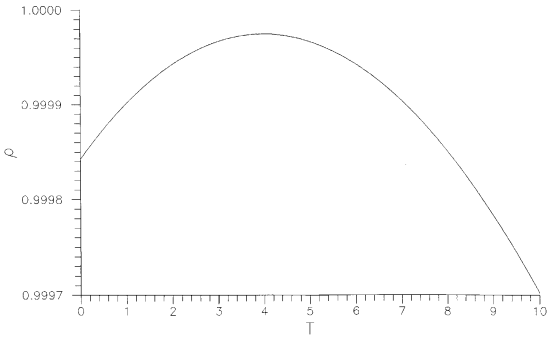

Fig. 1. Variation of water density in the 10–0 °C region.

decreases from 3.98 to 0 °C. The objective of the present paper is to present results for laminar free-convection of pure and saline water along a vertical isothermal plate with uniform blowing or suction in the temperature range between 20 and 0 °C, taking into account the temperature-dependence of viscosity and thermal conductivity as well as the non-linearity between density and temperature.

2. The mathematical model

Consider laminar free-convection along a vertical isothermal plate placed in a calm environment with u and v denoting, respectively, the velocity components in the x and y direction, where x is vertically upwards and y is the coordinate perpendicular to x. The flow is assumed to be steady, of the boundary layer type. The governing equations of this flow with Boussinesq approximations are:

$$\text{continuity equation}: \quad \frac{\partial u}{\partial x}+\frac{\partial v}{\partial y}=0, \tag{1}$$

momentum equation :

$$u\frac{\partial u}{\partial x}+v\frac{\partial u}{\partial y}=\frac{1}{\rho}\frac{\partial}{\partial y}\left(\mu\frac{\partial u}{\partial y}\right)-\frac{\rho-\rho_a}{\rho_a}g, \tag{2}$$

$$\text{energy equation}: \quad u\frac{\partial T}{\partial x}+v\frac{\partial T}{\partial y}=\frac{1}{\rho c_p}\frac{\partial}{\partial y}\left(k\frac{\partial T}{\partial y}\right), \tag{3}$$

where T is the water temperature, ρ and ρ_a are the local and ambient water density, μ is the dynamic viscosity, k is the thermal conductivity and c_p is the specific heat. The density of saline water is a function of temperature, salinity and pressure. In this paper the known from Oceanography International Equation of State for Seawater [6,18] is used for the calculation of density. This equation is valid for temperatures from -2 to 40 °C, salinities from 0‰ to 40‰ and pressures from 1 to maximum oceanic pressure in bars. In this work all calculations have been made for atmospheric pressure, that is for 1 bar.

In the boundary layer equations the dynamic viscosity, thermal conductivity and specific heat of water are included and must be calculated for each situation. For the calculation of saline water dynamic viscosity $\mu(T,s,p)$ the formula proposed by Matthaus was used (see [9]). The equation is valid for $0\ ^\circ\text{C}\leqslant T\leqslant 30\ ^\circ\text{C}$, $0‰\leqslant S\leqslant 36‰$ and 1–1000 bars but for larger ranges of T, s and p a slightly greater error is produced. The thermal conductivity was calculated from a formula proposed by Caldwell and the specific heat from a formula proposed by Bromley et al. (see [9]). The above formulae are valid for oceanic conditions.

The following boundary conditions were applied:

at

$$y=0: \quad u=0, \quad v=v_0, \quad T=T_0$$

as

$$y\to\infty \quad u=0, \quad T=T_a,$$

where v_0 is the fluid velocity normal to plate. Positive v_0 corresponds to blowing and negative to suction. T_0 is the plate temperature and and T_a is the ambient fluid temperature.

Eqs. (1)–(3) represent a two-dimensional parabolic flow. Such a flow has a predominant velocity in the streamwise coordinate which in our case is the vertical direction. In these flows convection always dominates the diffusion in the streamwise direction. This is expressed by the absence of streamwise velocity diffusion term in the momentum equation. In this kind of flows no reverse flow is accepted in the predominant direction. The solution of this problem in the present work is obtained by the finite difference method described by Patankar [15].

In the numerical solution of the boundary layer problems the calculation domain must always be at least equal or wider than the boundary layer thickness. However, it is known that the boundary layer thickness increases with x. If a Cartesian grid, formed by lines of constant x and y is chosen, the number of grid points within the boundary layer for small values of x, where the boundary layer is thin, is small and the computational accuracy is low. If the mesh length is reduced to have more points in the boundary layer at small x, the grid points at large x become excessive. Therefore, it would be desirable to have a grid which conforms to the actual shape of the boundary layer. In this work an expanding grid has been used (Fig. 2) according to the following relation:

$$y_{out}=y_0+cx, \tag{4}$$

where y_{out} is the outer boundary, c is the spreading rate of the outer boundary and x is the distance at the current step. The appropriate value of c has been found to be 0.15. The forward step size increases in proportion to the width of the calculation domain and the lateral cells are distributed uniformly. In this work the forward step was 1% of the outer boundary and a total of 300 lateral grid cells have been used. These values have been found by trial and error. For more information about the expanding grid, see [8]. Calculations were made on a DEC ALPHA 7000 computer using quadruple precision accuracy.

The momentum and energy equations have the following general form:

$$\rho u\frac{\partial\varphi}{\partial x}+\rho v\frac{\partial\varphi}{\partial y}=\frac{\partial}{\partial y}\left(\Gamma\frac{\partial\varphi}{\partial y}\right)+S, \tag{5}$$

where Γ is the diffusion coefficient and S is the source term. In the momentum equation the diffusion coefficient is equal to dynamic viscosity and in the energy equation equal to k/c_p. In the energy equation the

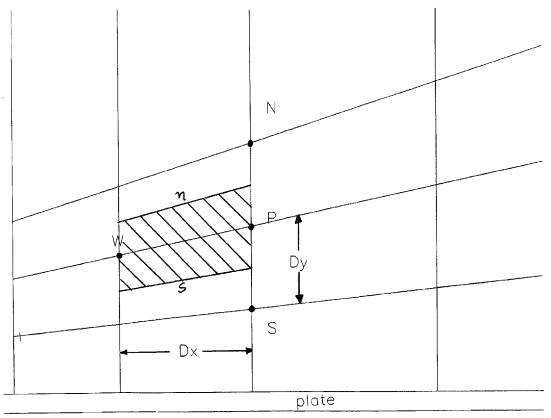

Fig. 2. Calculation domain.

source term is zero. The above differential equation is discretized directly and we have the following algebraic linear equation [15]:

$$a_P\varphi_P = a_W\varphi_W + a_N\varphi_N + a_S\varphi_S + b, \tag{6}$$

where

$$a_W = \frac{\Gamma_w\Delta y}{\Delta x} + (\rho u)_w\Delta y, \tag{7}$$

$$a_N = \frac{\Gamma_n\Delta x}{\Delta y} - (\rho v)_n\Delta x, \tag{8}$$

$$a_S = \frac{\Gamma_s\Delta x}{\Delta y} + (\rho v)_s\Delta x, \tag{9}$$

$$b = S\Delta x\Delta y, \tag{10}$$

$$a_P = a_W + a_N + a_S. \tag{11}$$

Eq. (6) can be written as follows:

$$-a_N\varphi_N + a_P\varphi_P - a_S\varphi_S = a_W\varphi_W + b. \tag{12}$$

The solution procedure starts with a known distribution of velocity and temperature at the plate edge and marches in the vertical direction. Flat initial velocity and temperature profiles were assumed. These profiles were used only to start the computations and their shape had no influence on the results which were taken far downstream of the edge. The coefficients a_N, a_P, a_S and the right-hand side term in the above equation are considered known in the current position because they are calculated using upstream known values. For example, let us consider the discretized momentum equation in the second grid line (the first grid line is located at the plate edge). The coefficient a_N is

$$a_N = \frac{\mu_n\Delta x}{\Delta y} - (\rho v)_n\Delta x \tag{13}$$

and is calculated using the values of μ, ρ and v from the first line. The dynamic viscosity is calculated using the Matthaus formula while the density is calculated using the International Equation of State for Seawater. The temperature used for the above calculations is taken from the initial temperature profile. The value of v in the first line in zero. The right-hand side term $a_W\varphi_W + b$ is also known. The coefficient a_W is calculated from values at the first line like a_N and φ_W is the velocity at the first line. The quantity b which represents the source term of the momentum equation and includes the density is calculated also at the first line using the International Equation of State for Seawater and temperatures of the first line.

If we have m points along each grid line we have $m-2$ equations similar to Eq. (12) from point 2 to point $m-1$. Point 1 is located at the plate and point m is far away from the plate where – the ambient conditions prevail. Velocities $u(1)$ and $u(m)$ are always zero. After writing the $m-2$ equations along the grid line we have a system of $m-2$ linear equations which has a tridiagonal form and the solution is obtained using the tridiagonal matrix algorithm (TDMA). Solving the above system we have the values of vertical velocity in the second line. The next step is the calculation of the cross-stream velocities v in the second line from the continuity Eq. (1). It should be noted here that the cross-stream velocity at the plate is v_0 so we have always $v(1) = v_0$. The third step is the calculation of the temperatures in the second line using the discretized equations of the energy equation. Now the coefficient a_N is

$$a_N = \frac{k_n\Delta x}{c_{\mathrm{p}}\Delta y} - (\rho v)_n\Delta x \tag{14}$$

and is calculated using the values of k, c_{p}, ρ and v from the first line. The thermal conductivity is calculated from the Caldwell formula and the specific heat from the Bromley formula. The boundary conditions for the energy equation is $T(1) = T_0$ and $T(m) = T_{\mathrm{a}}$. After the calculation of u, v and T in the second line the procedure is repeated at the third line taking into account as upstream values those calculated at the second line.

3. Results and discussion

It has been established that the problem of free-convection along a heated vertical plate with blowing or suction admits similarity solution only when the wall temperature and the transpiration velocity varies with x. For the more realistic case of isothermal plate with uniform blowing or suction considered in this paper no similarity solution exists. The two governing variables for this problem is the pseudo-similarity variable n and the streamwise non-dimensional variable ξ (injection parameter) defined as [16]

$$n = \frac{y}{x}\left[\frac{Gr_x}{4}\right]^{1/4}, \tag{15}$$

$$\xi = \frac{v_0 x}{v}\left[\frac{Gr_x}{4}\right]^{-1/4}, \tag{16}$$

where Gr_x is the local Grashof number and v is the fluid kinematic viscosity. As was mentioned before, in this work the water physical properties are handled as functions of temperature. This means that the kinematic viscosity v is variable across the boundary layer. In Eq. (16) we use the kinematic viscosity that corresponds to average temperature between the wall and the free stream. Thus we have

$$\xi = \frac{v_0\rho_{\mathrm{f}}}{\mu_{\mathrm{f}}}\left[\frac{Gr_x}{4}\right]^{-1/4}, \tag{17}$$

where ρ_f and μ_f is the film density and film dynamic viscosity both calculated at film temperature $(T_0 + T_a)/2$ [16]. The injection parameter ξ is positive for blowing and negative for suction. In the classical analysis with linear relationship between density and temperature the local Grashof number is defined as

$$Gr_x = \frac{gx^3\beta(T_a)(T_0 - T_a)}{\nu^2} \tag{18}$$

where $\beta(T_a)$ is the fluid thermal expansion coefficient taken at ambient temperature. The above Grashof number is unsuitable for water free-convection at low temperatures due to non-linear relationship between density and temperature. For example, when the ambient temperature corresponds to density extremum, the $\beta(T_a)$ coefficient becomes zero and the Grashof number becomes zero, too. In this case no similarity variable n can be defined. Therefore, the following Grashof number is further used

$$Gr_x = \frac{g\rho_f^2 x^3}{\mu_f^2}\frac{\rho_a - \rho_0}{\rho_a}, \tag{19}$$

where ρ_0 is the water density at the wall. The kinematic viscosity $(\nu = \mu/\rho)$ is again calculated at film temperature $(T_0 + T_a)/2$.

The problem of laminar free-convection over a vertical isothermal impermeable plate (zero blowing and suction) with constant μ and k and non-linear density–temperature relationship admits similarity solution [14]. The above problem is a special case of the more general problem treated in the present paper. Consequently the quantities used in the similarity analysis should be valid also for the porous plate. The vertical velocity is given by

$$u = \frac{2\mu}{x\rho}[Gr_x]^{1/2} f' \tag{20}$$

or in non-dimensional form as

$$f' = \frac{ux\rho}{2\mu}[Gr_x]^{-1/2}. \tag{21}$$

In the above equation μ and ρ are handled as variables across the boundary layer. A profile of the velocity f' has zero value at plate and far away from the plate and a maximum value f'_{max} in the intermediate region. The second derivative of f' with respect to n is

$$f'' = \frac{\rho x^2}{\mu\sqrt{2}}[Gr_x]^{-3/4}\left(\frac{\partial u}{\partial y}\right) \tag{22}$$

and the value of f'' at the plate is

$$f''(0) = \frac{\rho_0 x^2}{\mu_0\sqrt{2}}[Gr_x]^{-3/4}\left(\frac{\partial u}{\partial y}\right)_{y=0}. \tag{23}$$

This quantity is used for the calculation of the wall shear stress. Another useful quantity in this program is the wall heat flux $\varphi'(0)$ that is the derivative of the non-dimensional temperature at plate. Taking the derivative of the non-dimensional temperature $\varphi = (T - T_a)/(T_0 - T_a)$ with respect to n we have

$$\varphi'(0) = \frac{x}{T_0 - T_a}\left[\frac{Gr_x}{4}\right]^{-1/4}\left[\frac{\partial T}{\partial y}\right]_{y=0}. \tag{24}$$

In the present work the above quantities have been calculated as follows. As mentioned before the numerical method used is a space marching technique giving the downstream velocity and temperature profiles using the known upstream profiles. At every downstream position viscosity, thermal conductivity, specific heat and density are calculated at each grid point across the boundary layer from the calculated temperature profile using the above mentioned formulae. Then the Grashof number was calculated from Eq. (19). The next steps were the calculation of variable n from Eq. (15) and the calculation of non-dimensional vertical velocity profile f' from Eq. (21). The f'_{max} was calculated from known values across the boundary layer. The $f''(0)$ was calculated from Eq. (23) and the $\varphi'(0)$ from Eq. (24). The derivatives $[\partial u/\partial y]_{y=0}$ and $[\partial T/\partial y]_{y=0}$ were calculated from the following equations:

Table 1
Numerical results of Parikh et al. [16] and the present method ($Pr = 0.70$)

ξ	Nu_x/Nu_x^*		
	Parikh et al. [16]	Present method	Difference (%)
−2.0	2.820	2.856	1.28
−1.0	1.805	1.806	0.06
0.0	1.000	1.000	0.00
+1.0	0.465	0.460	−1.08
+2.0	0.160	0.160	0.00

Table 2
Correspondence between the ambient Prandtl number and ambient temperature of pure water

T_a	Pr_a
20.00	6.99
15.00	8.01
10.00	9.31
5.00	10.99
3.98	11.40
3.00	11.80
2.00	12.24
1.00	12.70

$$\left[\frac{\partial u}{\partial y}\right]_{y=0} = \frac{u(2)-u(1)}{\Delta y}, \tag{25}$$

$$\left[\frac{\partial T}{\partial y}\right]_{y=0} = \frac{T(2)-T(1)}{\Delta y}, \tag{26}$$

where (1) is a grid point on the plate and (2) is an adjacent grid point along y.

The accuracy of the method was tested comparing the results with those of the classical free-convection problem over a vertical isothermal impermeable plate

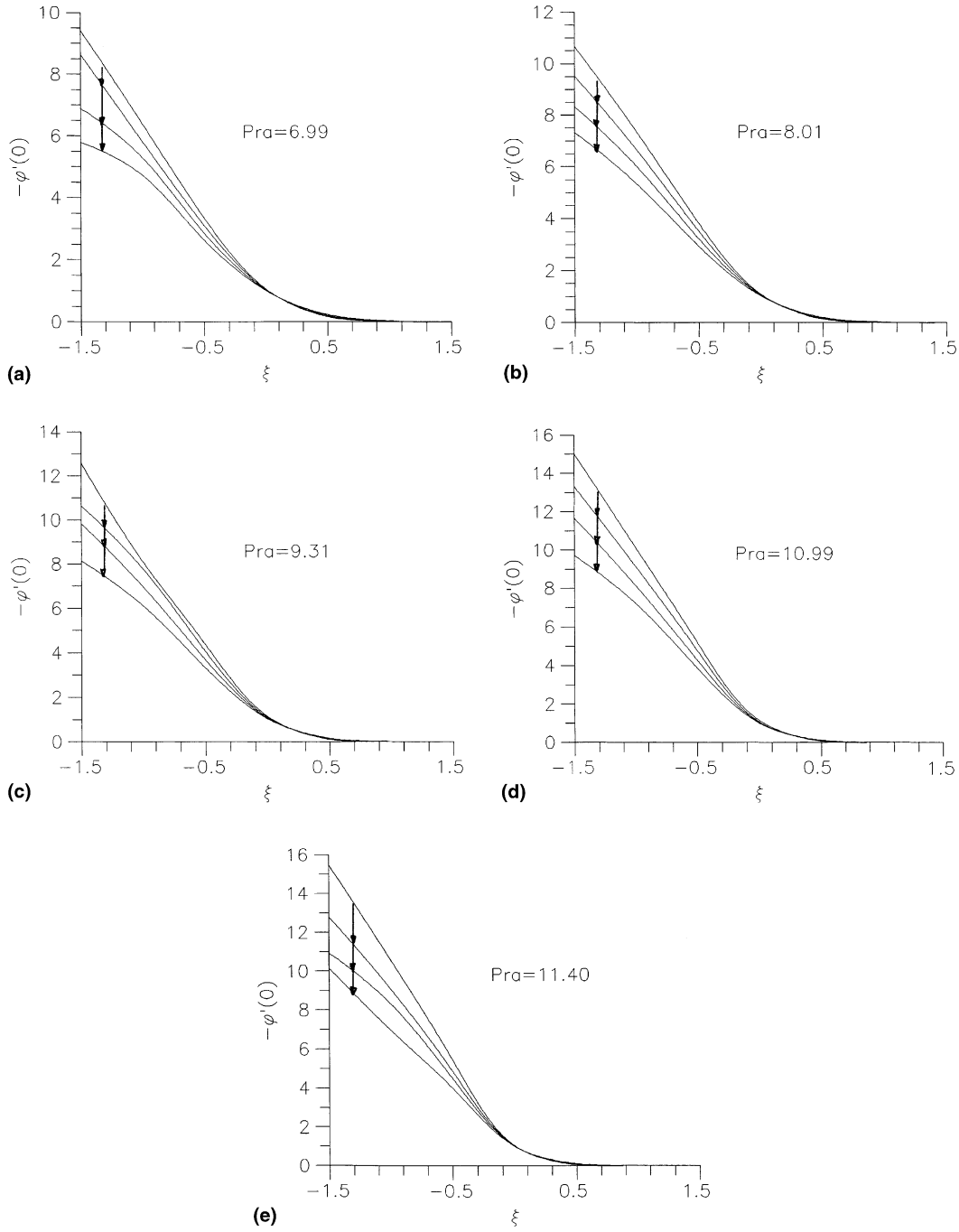

Fig. 3. Wall heat transfer for pure water as function of injection parameter for different temperature differences for each Pr_a number. Arrows show increasing ΔT: 1, 5, 10, 15 °C.

($\xi = 0$) for a fluid with constant viscosity and thermal conductivity and linear relationship between density and temperature. In the work of Gebhart [7] a complete table is given with data concerning the transport quantities of free-convection adjacent to vertical heated surfaces. This table was prepared by Krishnamurthy. For example, the quantities $-\varphi'(0)$, $f''(0)$ and $f'_{\max}$ for the isothermal case ($Pr = 6.7$) calculated with the present method were 1.0431, 0.4509 and 0.1334 and the corresponding results by Krishnamurthy were 1.0408, 0.4548 and 0.1335. Except of the above comparison the results of the present method including transpiration have been compared with those of Parikh et al. [16] for $Pr = 0.7$ and uniform transpiration velocities. Parikh et al. [16] presented numerical results for the ratio of transpiration Nusselt number Nu_x to the neutral Nusselt number Nu_x^* (zero blowing conditions, $\xi = 0$) for different values of injection parameter ξ. The above ratio is equal to $-\varphi'(0)/-\varphi'(0)^*$, where $-\varphi'(0)^*$ is the wall heat transfer which corresponds to an isothermal impermeable plate. The comparison is shown in Table 1.

The results of the present method have also been compared with those of Minkowycz and Sparrow [13] for $Pr = 5$ and 10 for water with constant viscosity and thermal conductivity (taken at ambient temperature) and linear relationship between density and temperature. The differences between the results varied from 0% to 2%.

As mentioned before the results produced in this work take into account both the non-linear relationship between density and temperature of water and the variation of viscosity and thermal conductivity with

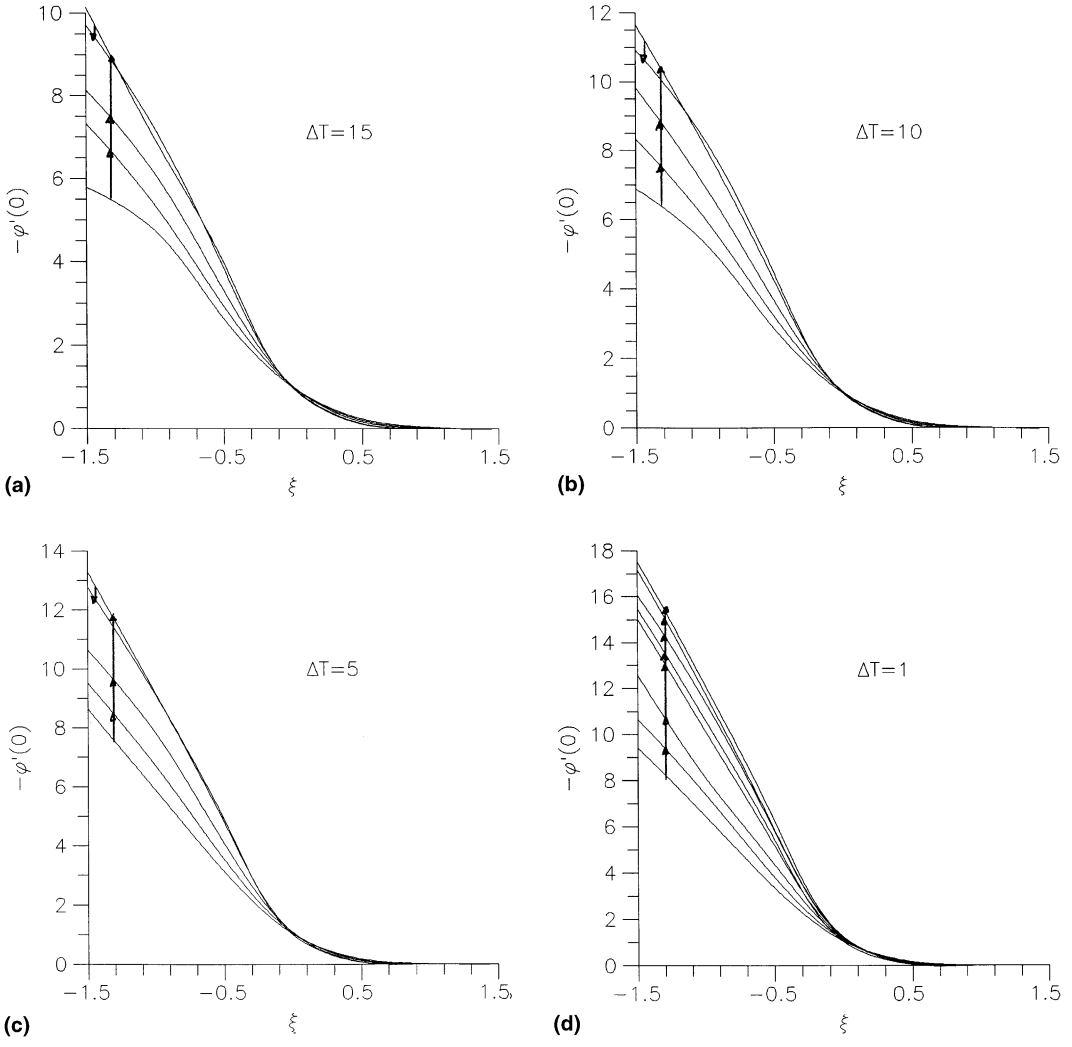

Fig. 4. Wall heat transfer for pure water as function of injection parameter for different Pr_a numbers for each temperature difference. Arrows show increasing Pr_a: 6.99, 8.01, 9.31, 10.99, 11.40 for $\Delta T > 1$ and 6.99, 8.01, 9.31, 10.99, 11.40, 11.80, 12.24, 12.70 for $\Delta T = 1$.

temperature. As it is expected the results depend on the temperature difference between the plate and the ambient water. For a given ambient water temperature and a constant Pr_a number calculated at this temperature, results have been produced for four temperature differences between the plate and the ambient water ($\Delta T = 1$, 5, 10 and 15 °C). The correspondence between the ambient Prandtl number and ambient water temperature is shown in Table 2.

For example, for ambient temperature 5 °C results were produced for plate temperature 6, 10, 15 and 20 °C. In the temperature range between 3.98 and 0 °C

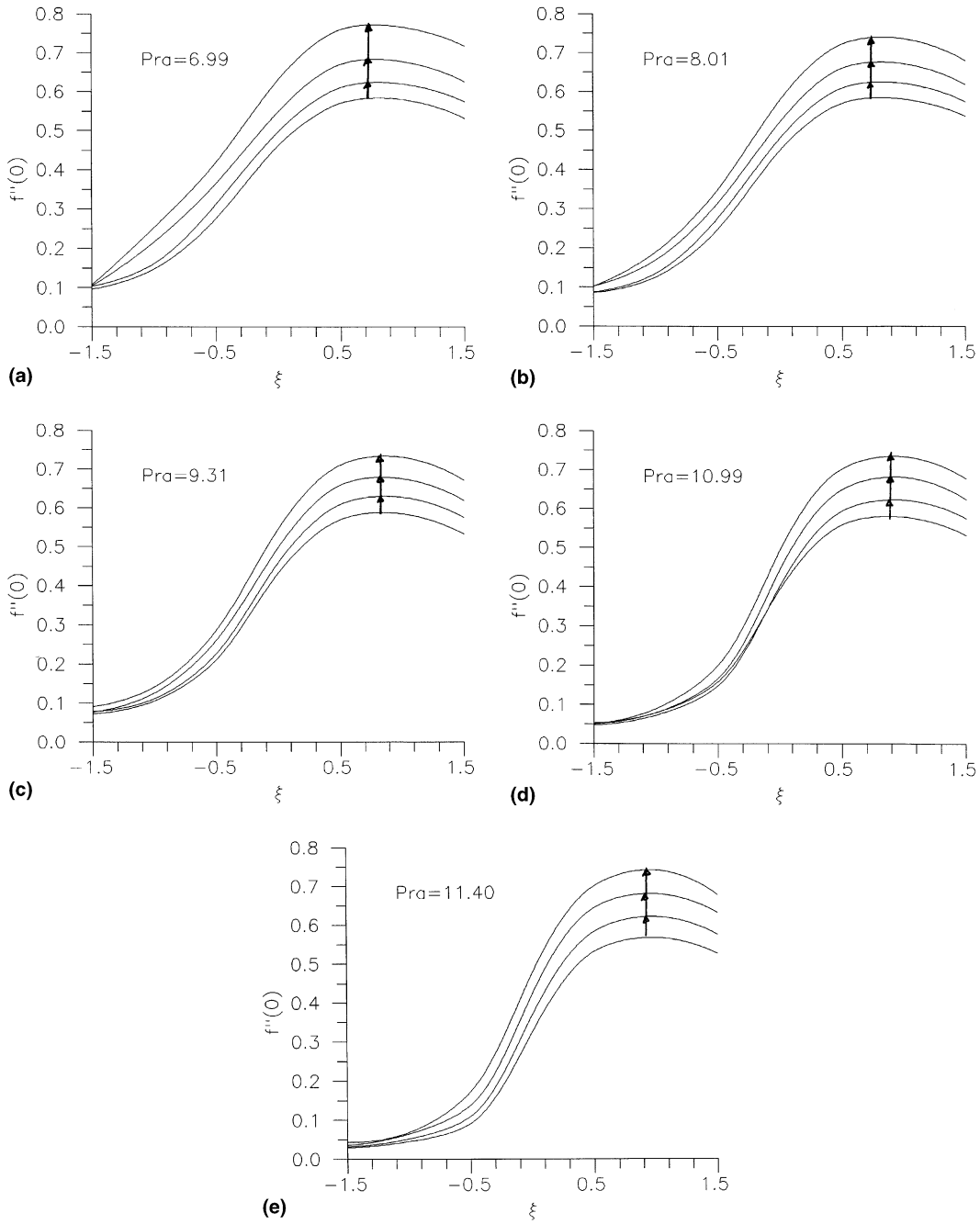

Fig. 5. Wall shear stress for pure water as function of injection parameter for different temperature differences for each Pr_a number. Arrows show increasing ΔT: 1, 5, 10, 15 °C.

results were produced only for $\Delta T = 1$ °C due to limited capability for multiple combinations. For example, for ambient temperature 3 °C results were produced for plate temperature 2 °C.

In the following figures the results of this work are presented. In Fig. 3 the wall heat transfer $-\varphi'(0)$ is shown as function of the injection parameter ξ for different temperature differences between the plate and the ambient water and different Pr_a numbers (6.99, 8.01, 9.31, 10.99, 11.40). The following conclusions can be drawn from this figure.

1. The wall heat transfer takes high values for large suction rates (negative ξ values) and decreases as the suction rate decreases. The $-\varphi'(0)$ value is much smaller for $\xi = 0$ (impermeable plate) and approaches a zero value as the blowing rate increases (positive ξ values).

2. The temperature difference between the plate and the ambient water plays an important role on wall heat transfer. For a suction rate equal to −1.5 and $Pr_a = 6.99$ the wall heat transfer takes a value of 9.412 for $\Delta T = 1$ °C and 5.790 for $\Delta T = 15$ °C. The first value is 62.56% greater than the second. Generally the wall heat

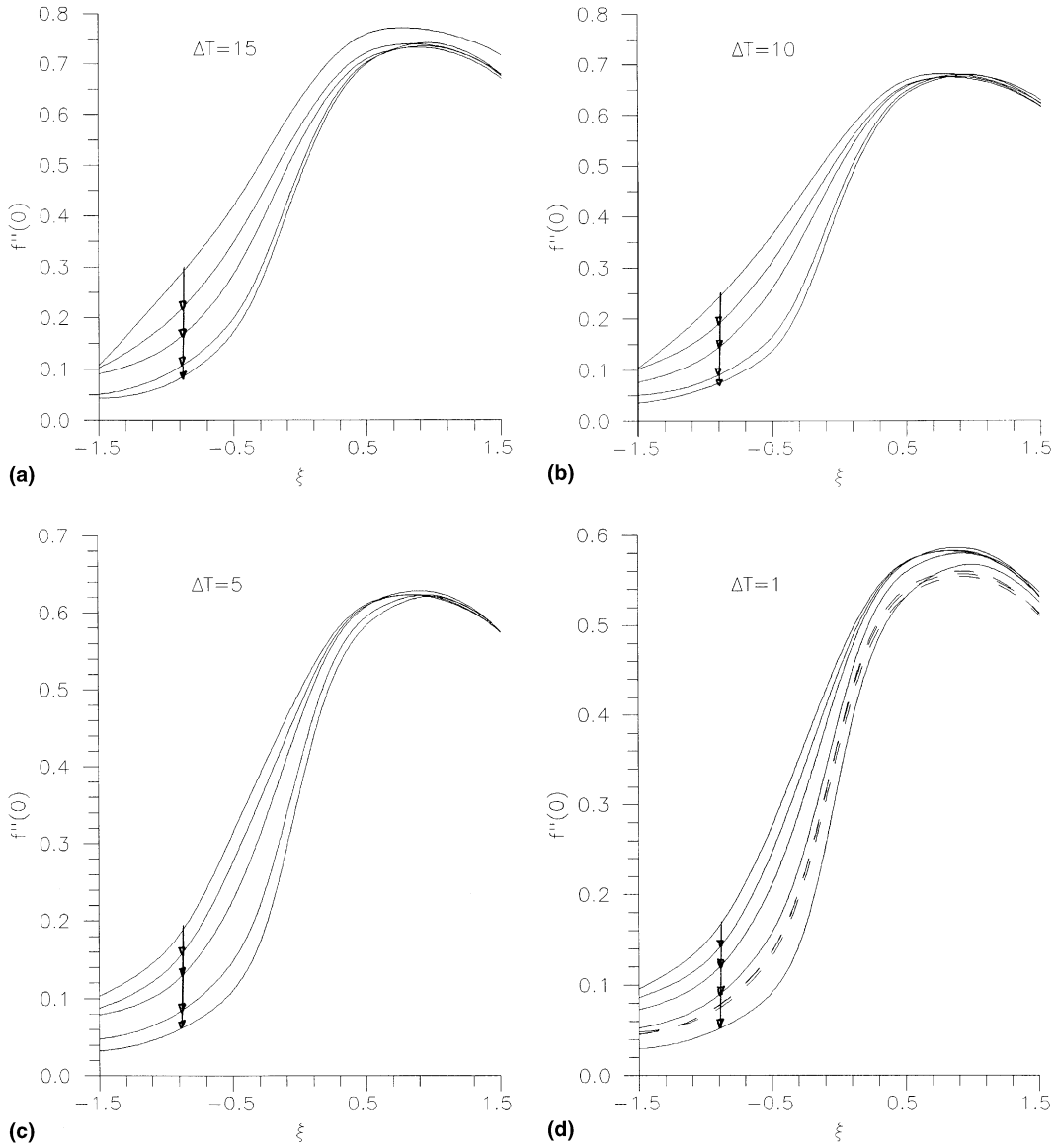

Fig. 6. Wall shear stress for pure water as function of injection parameter for different Pr_a numbers for each temperature difference. Arrows show increasing Pr_a: 6.99, 8.01, 9.31, 10.99, 11.40.

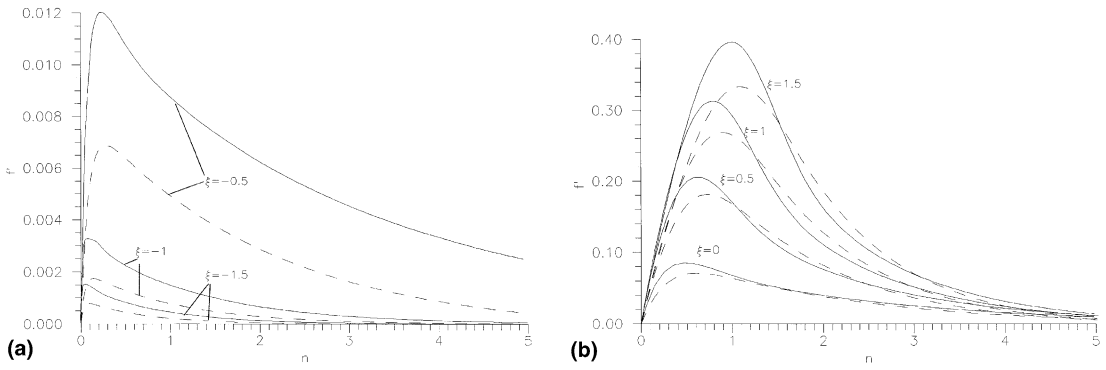

Fig. 7. Non-dimensional velocity profiles for pure water as function of injection parameter for $Pr_a = 11.40$. Solid lines correspond to $\Delta T = 15$ °C and dashed lines to $\Delta T = 1$ °C.

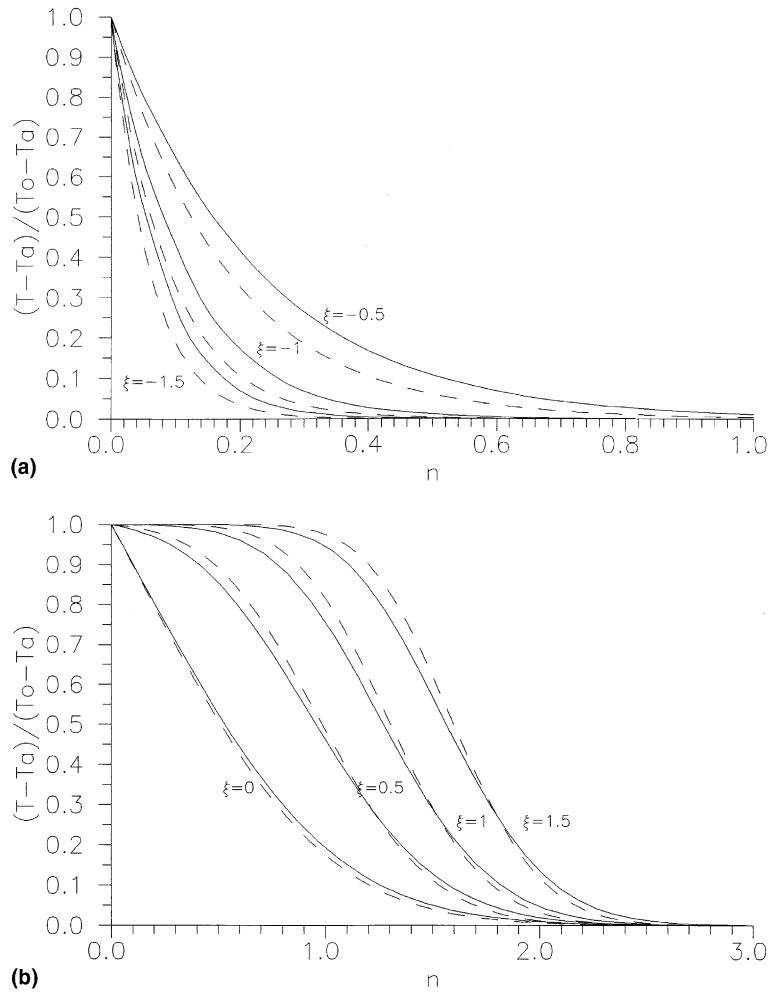

Fig. 8. Non-dimensional temperature profiles for pure water as function of injection parameter for $Pr_a = 11.40$. Solid lines correspond to $\Delta T = 15$ °C and dashed lines to $\Delta T = 1$ °C.

Table 3
Correspondence between the ambient Prandtl number and ambient temperature of saline water with salinity $s = 40‰$

T_a	Pr_a
20.00	7.28
15.00	8.31
10.00	9.60
5.00	11.21
0.00	13.25

transfer decreases as ΔT increases. When the temperature difference is small ($\Delta T = 1$ °C) the wall heat transfer increases almost linearly as the suction rate increases but this trend changes as ΔT increases. For a suction rate equal to -1.0 and $Pr_a = 0.70$ (air) the wall heat transfer is equal to 0.911 [16]. The corresponding value for water ($Pr_a = 6.99$, $T_a = 20$ °C, $\Delta T = 1°$ C) is 6.427 that is the water wall heat transfer is about seven times greater than that of air for this suction rate.

In Fig. 4 the wall heat transfer $-\varphi'(0)$ is shown as function of the injection parameter ξ for different Pr_a numbers for each temperature difference between the plate and the ambient water. The variation of wall heat transfer with ξ is the same as found before. The interesting point in these figures is the variation of $-\varphi'(0)$ with Pr_a number. For the first three Pr_a numbers (6.99, 8.01, 9.31) and for all ΔT values the heat transfer increases with Pr_a number increase in the suction side. In the blowing side the differences of $-\varphi'(0)$ are very small. For Pr_a numbers 10.99 and 11.40 and for $\Delta T = 15$, 10, and 5 °C the heat transfer differences are not clear except of a small region at high suction rates where the $Pr_a = 11.40$ heat transfer is lower than that of $Pr_a = 10.99$ in contrary to the general trend. When $\Delta T = 1$ °C the heat transfer increase with Pr_a number increase is valid for all Pr_a numbers (6.99–12.70).

In Fig. 5 the wall shear stress $f''(0)$ is shown as function of the injection parameter ξ for different temperature differences between the plate and the ambient water and different Pr_a numbers (6.99, 8.01, 9.31,10.99, 11.40). The following conclusions can be drawn from this figure.

1. The wall shear stress increases as the suction rate decreases and this increase continues on the blowing side where a maximum is obtained. This maximum occurs between $\xi = 0.5$ and $\xi = 1$. Further increase of blowing rate causes a decrease in wall shear stress. The occurrence of maximum shear stress at the blowing side has also been found by Merkin [12, Fig. 6(b)] for $Pr = 7.00$, isothermal plate ($m = 0$) and variable transpiration velocity ($v_0 = c_2 x^{-1/4}$). It should be noted here that the maximum shear stress for Pr $= 0.73$, isothermal plate ($m = 0$) and variable transpiration velocity ($v_0 = c_2 x^{-1/4}$) lies on the suction side according to results given by Eichhorn [5]. Combining the works of Merkin [12], Eichhorn [5] and the present one it is seen that the position of maximum shear stress moves from the suction side to the blowing side as the Pr number increases.

2. The temperature difference between the plate and the ambient water plays again an important role. The influence of ΔT decreases as the suction rate increases. For a blowing rate equal to 1 and $Pr_a = 6.99$ the wall shear stress takes a value of 0.580 for $\Delta T = 1°$ C and 0.765 for $\Delta T = 15$ °C. The second value is 31.90% greater than the first one. Generally the shear stress increases as ΔT increases. This trend is opposite to the one valid for wall heat transfer.

In Fig. 6 the wall shear stress is shown as function of the injection parameter ξ for different Pr_a numbers for each temperature difference between the plate and the ambient water. For the first five Pr_a numbers (6.99, 8.01, 9.31, 10.99, 11.40), for $\xi < 0.5$ and for all ΔT values there is a clear trend between the shear stress and the Pr_a number that is the shear stress decreases as the Pr_a increases. Another interesting point is the behavior of shear stress for ambient temperatures below the density extremum temperature ($T_a = 3.98$ °C). The shear stresses which correspond to Pr_a numbers 11.80, 12.24 and 12.70 (dashed lines on the last figure) do not follow the above trend and they lie between the $Pr_a = 10.99$ ($T_a = 5.00$ °C) and $Pr_a = 11.40$ ($T_a = 3.98$ °C) values. This is valid only for $\xi \leqslant 0.5$ while for $\xi > 0.5$ the shear stresses of the above three Pr_a numbers take the lowest values of all Pr_a numbers.

The present method, considering μ, k and ρ as functions of temperature, has also been used to produce results for $Pr_a = 10$ ($T_a = 7.78$ °C) and different ΔT in order to compare them with those of Minkowycz and Sparrow [13]. When $\Delta T = 1$ °C, the maximum difference between the results produced by the two methods was 5%. As the temperature difference increases the divergence increases, too. For example, when $\xi = -2.4$ and $\Delta T = 15$ °C the wall heat transfer and the wall shear stress calculated by the present method are 16.2873 and 0.04819 and the corresponding values given by Minkowycz and Sparrow [13] are 24.00 and 0.04166. The differences are 32.14% and 15.67%. For $\xi = 0$ (impermeable plate) and $\Delta T = 15$ °C the wall heat transfer and the wall shear stress calculated by the present method are 1.0208 and 0.5268 and the corresponding values given by Minkowycz and Sparrow [13] are 1.169 and 0.4192. The differences are 12.68% and 25.67%. The conclusion from this comparison is that, the results given by Minkowycz and Sparrow [13] for $Pr = 5$ and 10 are valid for water only when ΔT is small. For $Pr = 10$, ΔT should be below 1 °C.

The velocity and temperature profiles for $Pr_a = 11.40$ (maximum density temperature) and for $\Delta T = 1$ and 15 °C are presented in Figs. 7 and 8 for different values of injection parameter ξ. The effect of blowing is to increase the maximum velocity and shift its location far-

ther away from the wall. This shift is accompanied by an increase of the inclination of the velocity profile along the normal to the plate but only for $\xi \leqslant 1$. For stronger blowing rates, although the maximum velocity continues to move away from the plate, the corresponding profile inclination decreases. This means that the wall shear stress also decreases and therefore a maximum shear stress occurs in this region. This result is in accordance with the maximum shear stress found in Figs. 5 and 6. There are some other interesting points in velocity

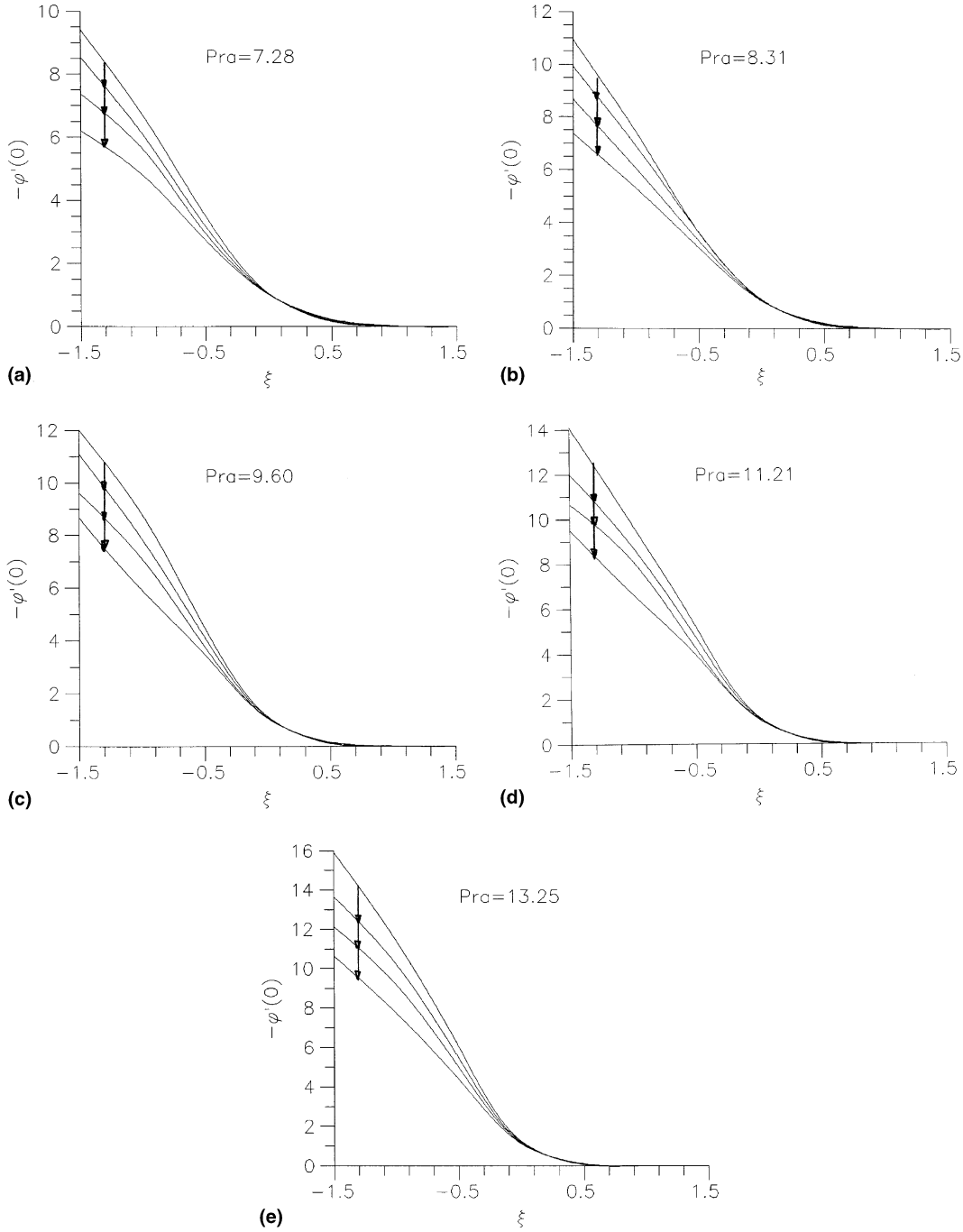

Fig. 9. Wall heat transfer for saline water ($s = 40‰$) as function of injection parameter for different temperature differences for each Pr_a number. Arrows show increasing ΔT: 1, 5, 10, 15 °C.

profile figures. The temperature difference between the plate and the ambient water plays an important role. Generally the maximum velocity increases as ΔT increases. For a suction rate equal to −0.50 the maximum velocity takes a value of 0.0069 for $\Delta T = 1$ °C and 0.0131 for $\Delta T = 15$ °C. The second value is 1.90 times greater than the first one. For a blowing rate equal to 1.50 the maximum velocity takes a value of 0.3330 for $\Delta T = 1$ °C and 0.3955 for $\Delta T = 15$ °C. The second value is 18.77% greater than the first one. From Fig. 8 it is seen that as the blowing rate increases the temperature profiles become wider and the boundary layer thickness

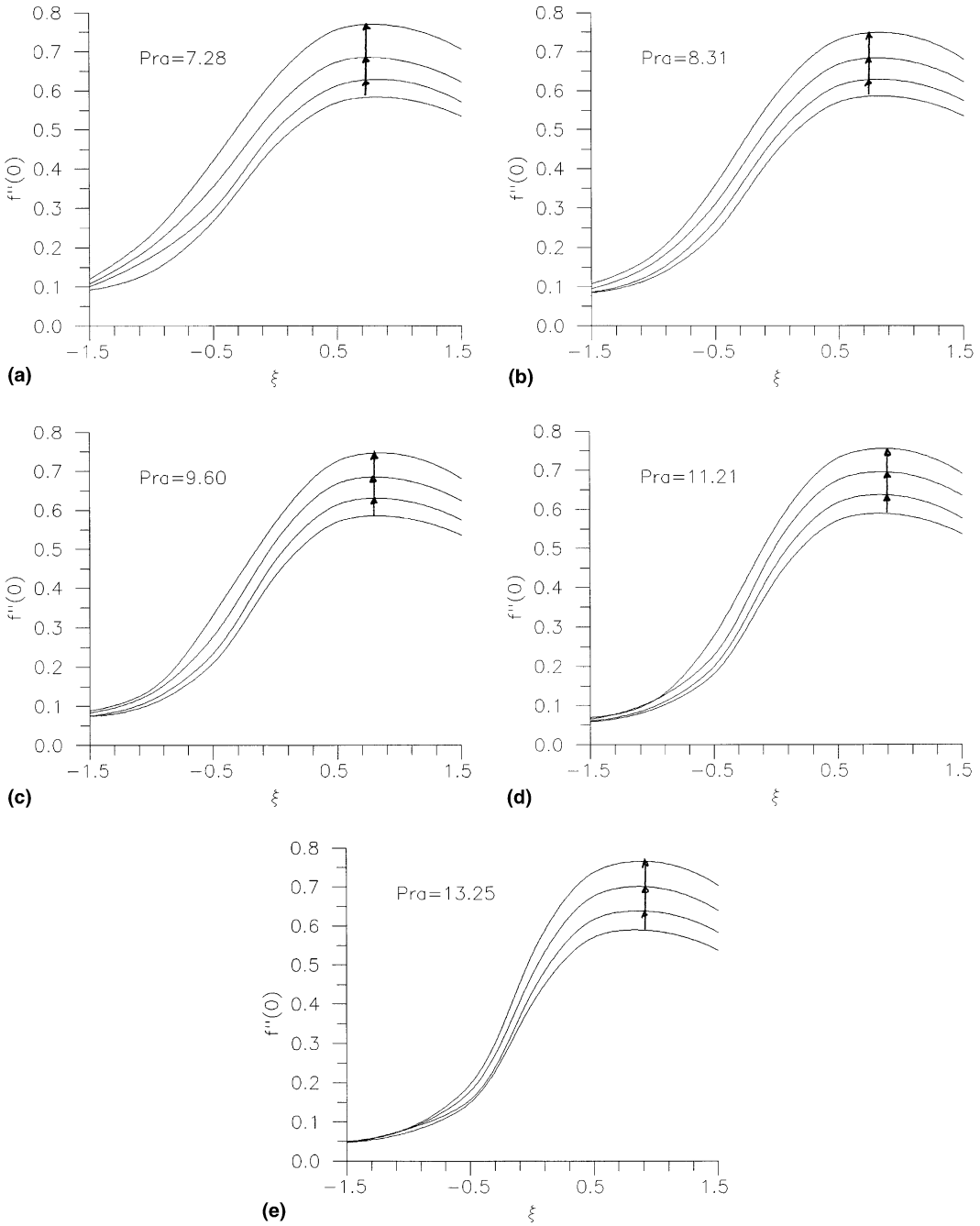

Fig. 10. Wall shear stress for saline water ($s = 40‰$) as function of injection parameter for different temperature differences for each Pr_a number. Arrows show increasing ΔT: 1, 5, 10, 15 °C.

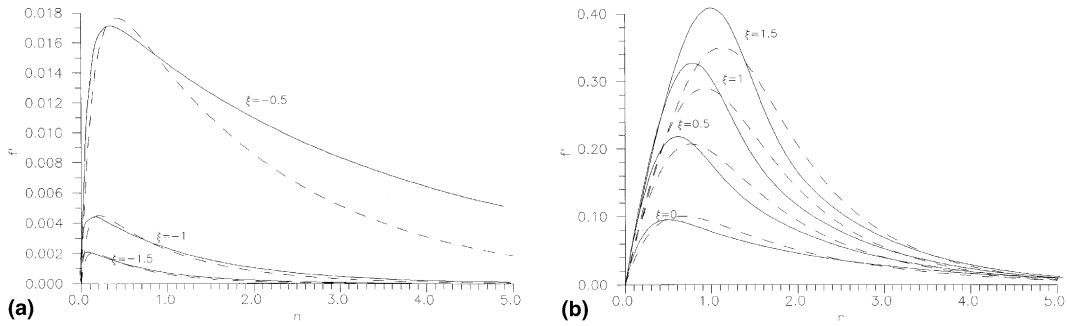

Fig. 11. Non-dimensional velocity profiles for saline water ($s = 40‰$) as function of injection parameter for $Pr_a = 13.25$. Solid lines correspond to $\Delta T = 15$ °C and dashed lines to $\Delta T = 1$ °C.

increases. The profiles that correspond to $\Delta T = 1$ °C have greater inclination than those of $\Delta T = 15$ °C at the suction side while the $\Delta T = 1$ °C inclination is smaller than that of $\Delta T = 15$ °C at the blowing side.

Following the above mentioned procedure results were also produced for saline water free-convection with constant salinity throughout the boundary layer equal to 40‰. The results are different from those of

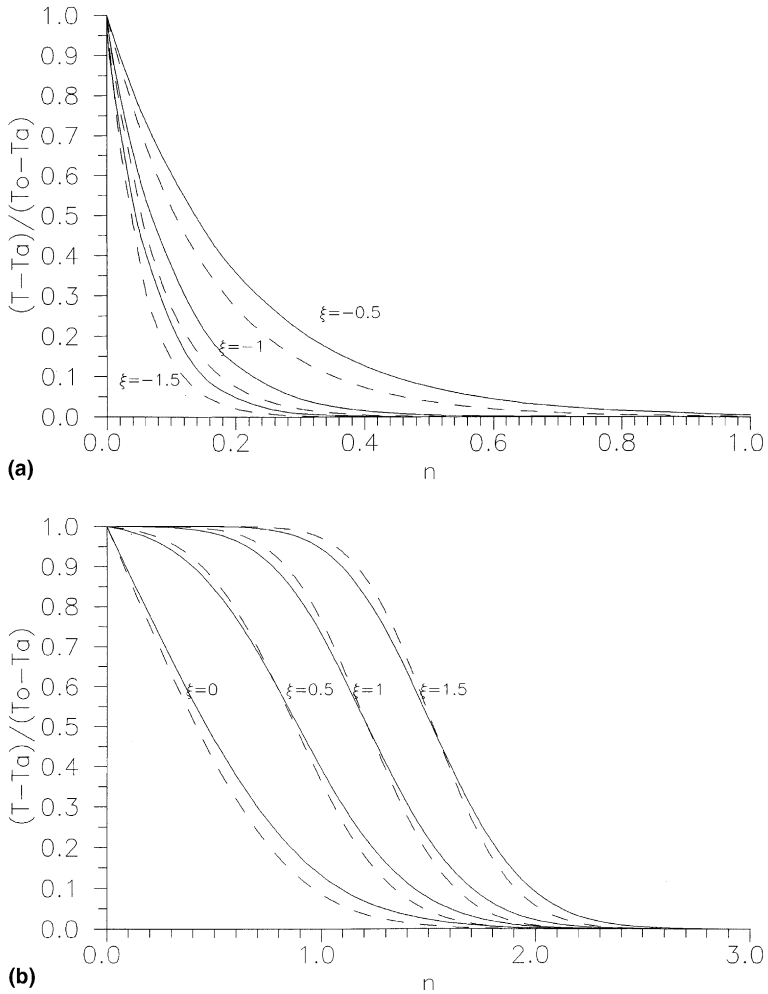

Fig. 12. Non-dimensional temperature profiles for saline water ($s = 40‰$) as function of injection parameter for $Pr_a = 13.25$. Solid lines correspond to $\Delta T = 15$ °C and dashed lines to $\Delta T = 1$ °C.

pure water because salinity influences the kinematic viscosity, thermal diffusivity and density and consequently the source term of momentum Eq. (2). It should be mentioned here that maximum density temperature is a function of salinity (for constant pressure) and this temperature decreases as the salinity increases. The maximum density temperature is 0 °C for salinity equal to 18.62‰ while this temperature is negative for greater salinities. The results produced in this work concern ambient temperatures in the range between 20 and 0 °C. Consequently no density extremum is included in this range for $s = 40‰$. The correspondence between the ambient Prandtl number and ambient saline water ($s = 40‰$) temperature is shown in Table 3.

In Figs. 9 and 10 the wall heat transfer $-\varphi'(0)$ and the wall shear stress $f''(0)$ are shown as function of the injection parameter ξ for different temperature differences between the plate and the ambient water and different Pr_a numbers (7.28, 8.31, 9.60, 11.21, 13.25). The velocity and temperature profiles for $Pr_a = 13.25$ and for $\Delta T = 1$ and 15 °C are presented in Figs. 11 and 12 for different values of injection parameter ξ. In general, the trends identified in pure water are valid also in saline water although the absolute values are different.

4. Conclusions

In this paper, the problem of pure and saline water free convection along a vertical isothermal plate with uniform transpiration has been investigated with the finite difference solution of the boundary layer equations. Results have been produced for the temperature range between 20 and 0 °C. The International Equation of State for Seawater is used for the calculation of the buoyancy force and the viscosity and thermal conductivity have been considered variable during the solution procedure. The major findings from the present study can be summarized as follows:

1. The temperature difference between the plate and the ambient water has a significant influence on all variables of the problem that is the wall heat transfer, the wall shear stress and the velocity and temperature profiles.
2. The maximum wall shear stress occurs in blowing when the fluid is water and in suction when the fluid is air.
3. In general, the wall heat transfer increases as the Pr number increases.
4. The wall shear stress decreases with the Pr number increase but this trend changes for ambient temperatures below the density extremum temperature.
5. The results of saline water are qualitatively the same as those of pure water although the arithmetic values are different.

References

[1] H.J.H. Brouwers, The film model applied to free convection over a vertical plate with blowing or suction, Int. J. Heat and Mass Transfer 35 (1992) 1841–1844.

[2] H.J.H. Brouwers, A film model for free convection over a vertical porous plate with blowing or suction, Warme- und Stoffübertragung 29 (1993) 17–26.

[3] M.A. Chaudhary, J.H. Merkin, The effects of blowing and suction on free convection boundary layers on vertical surfaces with prescribed heat flux, J. Eng. Math. 27 (1993) 265–292.

[4] J.F. Clarke, Transpiration and natural convection: the vertical-flat-plate problem, J. Fluid Mech. Part 1 57 (1973) 46–61.

[5] R. Eichhorn, The effect of mass transfer on free convection, J. Heat Transfer 82C (1960) 260–263.

[6] N.P. Fofonoff, Physical properties of seawater: a new salinity scale and equation of state for seawater, J. Geophys. Res. 90 (C2) (1985) 3332–3342.

[7] B Gebhart, Similarity solutions for laminar external boundary region flows, in: Natural Convection, Fundamentals and Applications, Hemisphere, Washington, DC, 1985.

[8] S.B. Jia,. Laminar jet issuing into stagnant surroundings, Computational Fluid Dynamics Unit, PDR/CFDU IC/15, Imperial College of Science and Technology, London, 1984.

[9] D.J. Kukulka, B. Gebhart, J.C. Mollendorf, Thermodynamic and transport properties of pure and saline water, Adv. Heat Transfer 18 (1987) 325–363.

[10] J.H. Merkin, Free convection with blowing and suction, Int. J. Heat Mass Transfer 15 (1972) 989–999.

[11] J.H. Merkin, The effects of blowing and suction on free convection boundary layers, Int. J. Heat Mass Transfer 18 (1975) 237–244.

[12] J.H. Merkin, A note on the similarity equations arising in free convection boundary layers with blowing and suction, ZAMP 45 (1994) 258–274.

[13] W.J. Minkowycz, E.M. Sparrow, Numerical solution scheme for local nonsimilarity boundary-layer analysis, Numer. Heat Transfer 1 (1978) 69–85.

[14] A. Pantokratoras, Laminar free convection of pure and saline water along a heated vertical plate, ASME J. Heat Transfer 121 (3) (1999) 719–722.

[15] S.V. Patankar, Numerical Heat Transfer and Fluid Flow, McGraw-Hill, New York, 1980.

[16] P.G. Parikh, R.J. Moffat, W.M. Kays, D. Bershader, Free convection over a vertical porous plate with transpiration, Int. J. Heat Mass Transfer 17 (1974) 1465–1474.

[17] E.M. Sparrow, R.D. Cess, Free convection with blowing or suction, J. Heat Transfer 81C (1961) 387–389.

[18] UNESCO, The Practical Salinity Scale 1978 and the International Equation of State of Seawater 1980. Tenth Report of the Joint Panel on Oceanographic Tables and Standards, UNESCO Technical Papers in Marine Science No. 36, UNESCO, Paris, France, 1981.

[19] M. Vedhanayagam, R.A. Altenkirch, R. Eichhorn, A transformation of the boundary layer equations for free convection past a vertical flat plate with arbitrary blowing and wall temperature variations, Int. J. Heat Mass Transfer 23 (1980) 1286–1288.